Published in final edited form as:
J Immunol. 2011 January 15; 186(2): 940–950. doi:10.4049/jimmunol.1000942.

Protein Kinase D Orchestrates the Activation of DRAK2 in Response to TCR-Induced Ca^{2+} Influx and Mitochondrial Reactive Oxygen Generation

Ryan H. Newton[*,†], **Sabrina Leverrier**[*,‡], **Sonal Srikanth**[§], **Yousang Gwack**[§], **Michael D. Cahalan**[*,‡], and **Craig M. Walsh**[*,†]

[*] Institute for Immunology, University of California, Irvine, Irvine, CA 92697

[†] Department of Molecular Biology and Biochemistry, University of California, Irvine, Irvine, CA 92697

[‡] Department of Physiology and Biophysics, University of California, Irvine, Irvine, CA 92697

[§] Department of Physiology, David Geffen School of Medicine, University of California, Los Angeles, Los Angeles, CA 90095

Abstract

DRAK2 is a serine/threonine kinase highly enriched in lymphocytes that raises the threshold for T cell activation and maintains T cell survival following productive activation. T cells lacking DRAK2 are prone to activation under suboptimal conditions and exhibit enhanced calcium responses to AgR stimulation. Despite this, mice lacking DRAK2 are resistant to organ-specific autoimmune diseases due to defective autoreactive T cell survival. DRAK2 kinase activity is induced by AgR signaling, and in this study we show that the induction of DRAK2 activity requires Ca^{2+} influx through the Ca^{2+} release-activated Ca^{2+} channel formed from Orai1 subunits. Blockade of DRAK2 activity with the protein kinase D (PKD) inhibitor Gö6976 or expression of a kinase-dead PKD mutant prevented activation of DRAK2, whereas a constitutively active PKD mutant promoted DRAK2 function. Knockdown of PKD in T cells strongly blocked endogenous DRAK2 activation following TCR ligation, implicating PKD as an essential intermediate in the activation of DRAK2 by Ca^{2+} influx. Furthermore, we identify DRAK2 as a novel substrate of PKD, and demonstrate that DRAK2 and PKD physically interact under conditions that activate PKD. Mitochondrial generation of reactive oxygen intermediates was necessary and sufficient for DRAK2 activation in response to Ca^{2+} influx. Taken together, DRAK2 and PKD form a novel signaling module that controls calcium homeostasis following T cell activation.

DRAK2 is an immunoregulatory serine/threonine kinase expressed highest in developing and mature lymphocytes (1, 2). Unlike other members of the death-associated protein kinase (DAPK) family to which this kinase belongs, DRAK2 does not directly promote apoptosis. Rather, DRAK2 is involved in setting the threshold for T cell activation, and its deficiency in T cells results in a response to suboptimal stimuli, ultimately leading to a defect in survival (3, 4). DRAK2 lacks the regulatory domains found within other members of the DAPK family, such as a death domain and calmodulin binding site found in DAPK1 (5).

Address correspondence and reprint requests to Dr. Craig M. Walsh, 3215 McGaugh Hall, University of California, Irvine, Irvine, CA 92697-3900. cwalsh@uci.edu.

Disclosures
The authors have no financial conflicts of interest.

Instead, its DAPK homology is restricted to the kinase domain, with a short N-terminal region subject to autophosphorylation, and a C terminus that appears to be involved in its nuclear localization following activation by PMA or UV irradiation in various carcinoma cell lines (6, 7). Although its effects on AgR-induced calcium mobilization are pronounced, the specific substrates it targets have remained elusive. In previous work, we established that DRAK2 is subject to activation and autophosphorylation following AgR stimulation (8). In an effort to understand how DRAK2 may be regulated during T cell activation, we have investigated signaling cascades induced by AgR stimulation that may be upstream of this kinase and necessary for its activation.

Protein kinase D (PKD), like DRAK2, belongs to the calcium/calmodulin-dependent superfamily of serine/threonine kinases. Three isoforms have been described, PKD1, 2, and 3, with a high degree of homology shared between them and similar mechanisms of activation (9). Various PKD isoforms have been shown to be indispensible for a number of cellular functions, including Golgi maintenance, vesicular trafficking, regulation of migration/motility, and apoptosis. PKD2 has been found to participate in IL-2 promoter regulation in T cells (10), although IL-2 has not been shown to directly activate PKD in T cells (11). Various transgenic mouse models have shown that PKD impacts T cell development (12), but a more detailed role in acute T cell signaling has not been described. Through its N-terminal cysteine-rich domain, PKD is responsive to the production of diacylglycerol and treatment with phorbol esters allowing membrane relocalization (13) and transphosphorylation events on its activation loop by various protein kinase C (PKC) family members (14). PKC-independent modes of activation have also been described in response to Gq-coupled receptor activation (15), as well as oxidative stress via tyrosine kinases Src and Abl (16, 17). Similar to DRAK2 (8), induction of PKD activity can be elicited by thapsigargin, a pharmacological agent that releases endoplasmic reticulum (ER)-stored calcium (18). Whereas a role for PKD in limiting mitochondrial uptake of calcium has been suggested (19), evidence is shown in this work that PKD, through its control of DRAK2 activity, is involved in limiting calcium mobilization upon activation in T cells.

Following engagement of their AgRs, store-operated capacitative calcium entry (SOCE) is triggered in T and B lymphocytes (20). This process requires the release of calcium from ER stores following phospholipase Cγ (PLCγ) activation and inositol 1,4, 5-triphosphate (IP_3) production. Luminal ER-Ca^{2+} depletion is sensed by STIM1, which migrates to ER plasma membrane junctions and activates calcium release-activated calcium (CRAC) channels formed from Orai1 channels, resulting in Ca^{2+} influx. High levels of calcium are required for NF-AT–driven gene expression, differentiation, and effector function following Ag-specific activation (21). PLCγ activation also leads to the engagement of diacylglycerol-dependent pathways necessary for lymphocyte function, such as those controlled by RasGRPs and both classical and novel PKC family members (22, 23). Control of calcium signaling is imperative for the prevention of aberrant T cell activation. Indeed, deficiencies in tyrosine phosphatases such as Src homology region 2 domain-containing phosphatase 1 and 2 and the 5′ inositol phosphatase SHIP1, which function to negatively regulate proximal immunoreceptor events, lead to enhanced calcium entry upon activation, potentially explaining the autoimmune phenotype observed in these mice (24, 25).

In this study, we show that PKD is involved in the regulation of DRAK2 activation, and that DRAK2 and PKD coordinate signals that limit activation-induced calcium entry in T cells. We show that disrupting PKD activity with the pharmacological inhibitor Gö6976, as well as knockdown of endogenous PKD, disrupts DRAK2 signaling. Additionally, we report that both calcium mobilization elicited by early TCR stimulation and extracellular calcium entry dependent on the CRAC channel component Orai1 are required for optimal induction of DRAK2 activity by PKD. PKD has been known to act as a sensor for reactive oxygen

species (ROS), and consistent with this, we observed that mitochondria-derived ROS (mROS) are necessary and sufficient for DRAK2 activation in response to extracellular calcium mobilization. Because DRAK2 is directly phosphorylated by PKD, our results provide a potential mechanism to describe PKD's role in eliciting DRAK2 kinase activity.

Materials and Methods

Cell culture, mice, Abs, and reagents

The mouse $CD4^+$ T cell clone D10 was obtained from L. Kane (University of California, San Diego). Cells were maintained in RPMI 1640 (Mediatech, Manassas, VA) supplemented with sodium pyruvate, nonessential amino acids, pennstrep-glutamine (Mediatech), 2-ME (Fisher Scientific, Pittsburgh, PA), and 20 U/ml human rIL-2. The human leukemic T cell line Jurkat (E6.1) was maintained in the same media, but without IL-2. The 293T cells were maintained in DMEM (Mediatech) supplemented as with RPMI 1640. Primary thymocytes were obtained from C57BL/6J mice and DRAK2-transgenic mice [previously described (26)], bred and maintained in accordance with the regulation of the Institutional Animal Care and Use Committee at the University of California, Irvine. Mice were used between 8 and 12 wk of age. Orai1 knockout mice used in this study were 6–7 wk old in an outbred, mixed genetic background. Generation and maintenance of these mice have been previously described (27). Abs for DRAK2, PKD1, P-PKD1(Ser^{916}), P-PKD1($Ser^{738/742}$), ERK1/2, P-ERK1/2, hemagglutinin, P-Ser^{12}, tubulin, and actin were obtained from Cell Signaling Technology (Danvers, MA). Anti–histone-H1 was obtained from Millipore (Billerica, MA). Anti-prohibitin was obtained from NeoMarkers (Fremont, CA). Alexa Fluor 488 goat anti-rabbit IgG was obtained from Molecular Probes, Invitrogen. Thapsigargin, BAPTA-AM, Gö6976, Gö6983, Ro-31-8425, fluphenazine, KN-93, SP-600125, and Mn (III) tetrakis (4-benzoic acid) porphyrin (MnTBAP) were obtained from EMD Chemicals (Gibbstown, NJ). Carbonyl cyanide *m*-chloro phenyl hydrazone (CCCP), butylated hydroxyanisole (BHA), *N*-acetyl- L-cysteine (LNAC), and PMA were obtained from Sigma-Aldrich (St. Louis, MO). EGTA was obtained from Fisher Scientific. The 2C11-biotin was obtained from eBioscience (San Diego, CA). Streptavidin-UNLB was obtained from Southern Biotechnology Associates (Birmingham, AL).

Recombinant protein purification

pGEX-2TK-DRAK2 (GST-DRAK2), GST-DRAK2-K62A, and GST-DRAK2-ΔC were cloned, as previously described (8). GST-tagged recombinant protein was purified from bacterial lysate using reduced glutathione-agarose beads (Sigma-Aldrich). Isopropyl 1-thio-β-D-galacto-pyranoside-induced BL21 cells were lysed in 50 mM Tris-HCl (pH 7.5), 300 mM NaCl, 1% Tween 20, 1% Triton X-100, 1 mg/ml lysozyme, and 1 mM PMSF for 30 min on ice. The lysate was subsequently spun for 20 min at 16,000 rpm and subjected to overnight binding with reduced glutathione-agarose beads. The beads were then washed with lysis buffer (without lysozyme). rGST-DRAK2 was eluted by incubating the beads for 20 min in 20 μM reduced glutathione (Sigma-Aldrich) diluted in 50 mM Tris-HCl (pH 7.5) and 150 mM NaCl.

In vitro kinase assays

rGST-PKD2 was obtained from ARP (Belmont, MA). Murine rDRAK2 was received from B. Wen (Genomics Institute of the Novartis Research Foundation, San Diego, CA). In vitro kinase assays with rDRAK2 were performed at 30°C for 20 min with kinase reaction buffer (10 mM Tris-HCl [pH 7.5], 10 mM $MgCl_2$, 3 mM $MnCl_2$), 20 μM ATP, 2 mM DTT, and 5 μCi [γ-^{32}P]ATP (GE Healthcare, Piscataway, NJ). Some reactions included 5 μg rabbit myosin L chain (MLC; Sigma-Aldrich) or myelin basic protein (MBP; Sigma-Aldrich) as a transphosphorylation substrate for DRAK2 or PKD2, respectively. For in vitro kinase assays

using GST-PKD2, kinase reaction buffer consisted of 25 mM MOPS, 12.5 mM β-glycerophosphate, 25 mM $MgCl_2$, 5 mM EGTA, 2 mM EDTA, 0.25 mM DTT, and 5 μCi [γ-^{32}P]ATP; assays were performed at 30°C for 20 min. Kinase reactions were terminated by the addition of Laemmli sample buffer. After boiling, the samples were separated by SDS-PAGE and visualized by autoradiography.

Retroviral and lentiviral transduction, transfections, and knockdown

pSM2c-shDRAK2, -shscrambled (Open Biosystems, Huntsville, AL) constructs were transfected into 293T cells, and retroviral supernatant was collected, as previously described (2). pLKO.1-shPKD2, -shScrambled constructs (laboratory of A. Toker, Addgene, Cambridge, MA, respectively) were transfected with plasmids VSVG and δ8.2 in 293T, and lentivirus was collected once 48 h posttransfection (following fresh media change 3 h posttransfection). Cells were spin-fected using retroviral or lentiviral supernatant and 5 μg/ml polybrene (Sigma-Aldrich) for 1 h at 1800 rpm, and incubated for 24 h at 37°C before selection for 2 d with puromycin (5 μg/ml in Jurkat T cells, 12 μg/ml in D10 T cells). Calcium mobilization assays were performed in D10 cells, as described below, following 24 h in media without puromycin. Jurkat T cells were stimulated and lysed for Western blot following 2-d selection with puromycin. Transfections in 293T cells were carried out using the calcium phosphate method. pcDNA3-HA-PKD1-K612W was obtained from the laboratory of D. Cantrell. pEGFP-PKD1-S738/742E was obtained from the laboratory of E. Rozengurt.

Flow cytometric calcium mobilization assays and single-cell intracellular calcium concentration imaging

D10 T cells were labeled in RPMI 1640 plus 2% FCS with 4.6 μM Fura red (Molecular Probes, Invitrogen, Carlsbad, CA), 3.4 μM Fluo-3 (Molecular Probes), and 0.02% pluronic (Molecular Probes) for 30 min at 37°C. Cells were washed with cold (unsupplemented) RPMI 1640. Samples were prewarmed for 15 min prior to analysis. Calcium mobilization was plotted as a ratio of Fluo-3: Fura red using the kinetics suite of FlowJo Software (Tree Star, Ashland, OR). Intracellular calcium concentration ($[Ca^{2+}]_i$) imaging was performed in purified primary T lymphocytes using the ratiometric probe fura 2. A total of 1×10^6 activated wild-type or Orai1$^{-/-}$ T cells was loaded with 2 μM fura 2-AM for 30 min at room temperature in culture medium, while adhering on poly(lysine-D)-coated coverslips. Loaded cells were washed five times with 2 mM Ca ringer solution (Ca2), mounted in a chamber permitting solution exchange by a syringe-driven perfusion system, and placed on the stage of an inverted Olympus IX81 microscope. Alternating 360 or 385 nm light was used to excite fura 2 and imaged $[Ca^{2+}]_i$ variation in individual cells. ER calcium stock was release with 1 mM thapsigargin for 5 min in a Ca-free media, and the CRAC-dependent calcium uptake was induced by addition of 2 mM Ca (Ca2) in the perfused media. Data were acquired and analyzed under control of METAFLUOR software (Molecular Devices, Downingtown, PA) and ORIGINPRO 7.5 software (OriginLab, Northampton, MA) and are expressed as means ± SEM.

Coimmunoprecipitation and blue-native PAGE

Cells were lysed in immunoprecipitation (IP) buffer (20 mM Tris-HCl [pH 7.4], 50 mM NaCl, 10 mM β-glycerophosphate, 50 mM NaF, 1% Triton X-100, 1 mM PMSF). A total of 300 μg lysate was precleared with protein A/G agarose (Calbiochem, EMD Chemicals) plus 2 μg rabbit IgG for 3 h, then incubated overnight with 3 μl anti-DRAK2 (150 μl lysate volume), followed by incubation with protein A/G agarose. Immunoprecipitate was washed four times in IP buffer, and then resolved by SDS-PAGE. Blue-native PAGE was carried out using the NativePAGE Gel system from Invitrogen. For standard cell lysis, prior to SDS-PAGE analysis, cells were lysed in 20 mM Tris-HCl (pH 7.4), 150 mM NaCl, 10 mM β-

glycerophosphate, 50 mM NaF, 1% Triton X-100, and 1 mM PMSF, plus aprotinin (Sigma-Aldrich) and phosphatase inhibitor mixtures I and II (Sigma-Aldrich).

Subcellular fractionation

To obtain nuclei, cells were lysed in hypotonic buffer (10 mM HEPES-KOH [pH 7.5], 10 mM KCl, 1.5 $MgCl_2$, 0.5 mM DTT, 0.5% Nonidet P-40, 1 mM PMSF) for 10 min on ice. Nuclei were pelleted at 3,000 rpm for 2 min, washed with hypotonic buffer (without Nonidet P-40), resuspended in lysis buffer (20 mM HEPES-KOH [pH 7.9], 400 mM NaCl, 0.2 mM EDTA, 1.5 mM $MgCl_2$, 0.5 mM DTT, 25% glycerol, 1 mM PMSF), and incubated on ice for 30 min with periodic vortexing. Supernatant containing nuclear protein was obtained by spinning at 13,200 rpm for 15 min at 4°. Mitochondrial, S-100, and P-100 fractions were prepared, as previously described (17).

Immunofluorescence labeling and fluorescence microscopy

Whole splenocytes were stained with 300 nM MitoTracker Red in RPMI 1640 unsupplemented for 30 min and then adhered to poly(L-lysine)-coated coverslips. Following treatment with thapsigargin or with vehicle, cells were fixed in 3% paraformaldehyde made in PBS for 20 min. Cells were then washed three times with PBS and blocked and permeabilized for 1 h at room temperature with PBS supplemented with 10% normal donkey serum and 0.1% Triton X-100. Following washes in PBS, cells were incubated with anti-DRAK2 diluted 1:100 in PBS supplemented with 5% BSA and 0.1% Triton X-100 overnight at 4°. Following washes in PBS, anti-rabbit Alexa Fluor 488 secondary Ab was diluted 1:1000 in PBS supplemented with 5% BSA and 0.1% Triton X-100 for 2 h at room temperature. Following washes in PBS, cells were mounted on glass slides using VectaShield Mounting medium with DAPI. Images were collected on a Zeiss Axiovert 200M using the Axiovision camera and software, and exported for manipulation in Photoshop 8.0.

Results

DRAK2 activity both requires and targets calcium influx upon lymphocyte activation

Previous work with DRAK2-deficient primary lymphocytes has revealed a role for DRAK2 in restricting calcium mobilization following AgR cross-linking (1, 2). Although these experiments supported the idea that DRAK2 acute signaling is involved in regulating calcium mobilization, we wanted to determine whether the augmented Ca^{2+} mobilization observed in DRAK2-deficient cells may be a result of altered T cell development, because DRAK2 is transcriptionally upregulated upon thymocyte maturation (2). We used a $CD4^+$ T cell line, D10.G4.1 (D10) (28), in which we achieved appreciable knockdown of DRAK2 using short hairpin RNA (Fig. 1*A*, *right panel*), to determine whether the DRAK2-deficient phenotype of enhanced calcium mobilization is recapitulated upon acute blockade of DRAK2 expression. D10 T cells expressing a scrambled short hairpin, or one specific for DRAK2, were stimulated with thapsigargin, an ER calcium store-depleting agent, in the presence of calcium-free media (Fig. 1*A*, *left panel*). Similar basal levels of intracellular calcium and store depletion were observed between knockdown and wild-type cells. Upon the addition of calcium following store depletion with thapsigargin, a striking increase in calcium entry was observed in DRAK2-depleted cells, indicating that DRAK2 negatively regulates SOCE. We note that this defect was revealed upon treatment with thapsigargin, which bypasses proximal TCR events to induce SOCE, and thus conclude that DRAK2 functions downstream of ER calcium release to modulate extracellular calcium influx.

To further understand the requirement for activation of DRAK2 in this negative feedback loop, calcium-chelating agents were used to interfere with both intracellular and

extracellular calcium levels. Addition of either BAPTA-AM or EGTA to chelate intracellular or extracellular calcium, respectively, blocked DRAK2 autophosphorylation on Ser^{12}, a previously demonstrated activation marker (8), in thapsigargin- and TCR cross-linking–induced D10 cells (Fig. 1*B*, 1*C*). Similarly, the effects of BAPTA-AM and EGTA are demonstrated in thapsigargin-treated thymocytes (Fig. 1*D*). Also, in accord with the requirement for calcium entry in eliciting the DRAK2 pathway, Jurkat T cells responded to thapsigargin with DRAK2 autophosphorylation only when calcium was present in the media, and not in nominally calcium-free media (Fig. 1*Ei*), indicating the usefulness of these cells, subsequently used for knockdown studies, for interrogating the signaling requirements of DRAK2. Likewise, in both primary thymocytes and D10 cells (Fig. 1*Eii*, 1*Eiii*, respectively), DRAK2 activation by thapsigargin depended on the presence of extracellular calcium. We note that in D10 cells, both EGTA and the use of calcium-free media led to only partial blockade of DRAK2 activation, whereas this blockade was complete in both Jurkat and primary thymocytes. It is possible that this difference emerges as the result of distinct magnitudes of intracellular calcium stores between these cells.

Influx of calcium upon T cell activation is largely a consequence of CRAC channel activity (29), in which conformational changes and oligomerization of the pore-forming subunit of the CRAC channel, Orai1, are induced by STIM1, an EF-hand containing ER resident calcium sensor (30). Interestingly, in Orai1 knockout mice, the defect in Ca^{2+} influx is markedly more pronounced in T cells that are no longer naive (i.e., after they have previously been activated) (31). Accordingly, we used activated T cells from wild-type and $Orai1^{-/-}$ mice to evaluate effects of Ca^{2+} signaling on DRAK2 activation (Fig. 2*A*). The defect in calcium seen in Orai1-deficient cells correlates well with a defect in DRAK2 activation (Fig. 2*B*), further demonstrating the requirement for calcium influx, as well as a dependence on CRAC channel activity, for DRAK2 function.

Identification of PKD as necessary for DRAK2 activation

Using inhibitors of various pathways involved in T cell activation and those elicited by thapsigargin, we carried out a small-scale screen to identify signaling pathways that may be required for DRAK2 activation. The PKC/PKD inhibitor Gö6976 uniquely and potently inhibited thapsigargin-induced DRAK2 autophosphorylation (Fig. 3*A*). To distinguish between a dependence on PKC versus PKD, we compared the effect of the pan-PKC inhibitor Gö6983, which is ineffective at PKD (PKCμ) inhibition at the concentration used, with the PKD inhibitor Gö6976 on DRAK2 Ser^{12} phosphorylation (27), and observed that Gö6983 was ineffectual at blocking DRAK2 signaling (Fig. 3*B*). Because PKD and DRAK2 belong to the same superfamily of calcium-calmodulin–regulated kinases, we sought to determine whether Gö6976 was able to directly block DRAK2 catalytic activity, or if this blockade was instead due to inhibition of PKD activity. Using in vitro kinase assays with recombinant PKD and DRAK2, autophosphorylation and transphosphorylation of MLC by DRAK2 were not affected by Gö6976 (Fig. 3*C*). In contrast, autophosphorylation and transphosphorylation of MBP by PKD were greatly reduced by the presence of Gö6976 (Fig. 3*C*), demonstrating specific blockade of PKD, but not DRAK2, by this inhibitor.

To further investigate a potential role for PKD in DRAK2 signaling, we used 293T cells as a heterologous system to express various mutants of PKD cotransfected with DRAK2. Because PKD is responsive to diacylglycerol production, and 293T cells do not exhibit the high level of SOCE that thapsigargin elicits in T cells to promote DRAK2 activation, we used the diacylglycerol mimetic PMA to elicit DRAK2 activation in 293T cells. Treatment with PMA did enhance DRAK2 autophosphorylation on Ser^{12} in 293T cells above basal levels (Fig. 4*A*). When coexpressed with a kinase-dead PKD mutant (KD-PKD1; PKD1-K612W) to act in a dominant-negative manner, basal levels of DRAK2 autophosphorylation were reduced, and PMA-induced DRAK2 autophosphorylation was greatly reduced as well.

Coexpression of DRAK2 and a constitutively active PKD mutant (CA-PKD1; PKD1-S738/742E) were sufficient to greatly enhance DRAK2 autophosphorylation, supporting the hypothesis that PKD catalytic activity promotes DRAK2 function. Further support of this hypothesis was provided through PKD knockdown experiments using Jurkat T cells, targeting PKD2 as the relevant isoform in this cell type (10). We obtained significant knockdown of PKD2 following infection of Jurkat cells with a lentivirus expressing a short hairpin RNA to human PKD2, but not with a scrambled hairpin lentivirus (Fig. 4*B*). We observed that DRAK2 activation induced by anti-CD3 cross-linking or thapsigargin was greatly diminished by PKD2 knockdown, demonstrating that PKD is required for DRAK2 activation. Unexpectedly, PMA did not lead to strong DRAK2 activation in these cells, although it did lead to induction of PKD autophosphorylation and ERK1/2 phosphorylation. These findings suggest that whereas DRAK2 is a target of PKD activity, its activation by PKD likely involves coordination of signaling, and possibly scaffolding, events that differs between cell types (see below).

DRAK2 interacts with activated PKD at mitochondria

Because our findings showed that PKD activity was necessary for DRAK2 autophosphorylation following calcium influx, we postulated that a direct interaction between DRAK2 and PKD may confer autocatalytic activity on DRAK2. Upon treatment with PMA in D10 cells, cells in which PMA does elicit DRAK2 activity, PKD coimmunoprecipitated with DRAK2 (Fig. 5*A*). We were not able to immediately observe the reverse coimmunoprecipitation in D10, potentially due to the nonimmunodepleting property of this Ab in conjunction with a high PKD/DRAK2 ratio (data not shown). However, using previously described DRAK2-transgenic thymocytes in which levels of DRAK2 are highly embellished (26), we were able to immunoprecipitate DRAK2 using anti-PKD (Fig. 5*B*). This interaction was enhanced upon stimulation with thapsigargin, further supporting the idea that activation of these kinases promotes their interaction. To gain more insight into this interaction, we used blue-native PAGE of lysates from D10 cells treated with PMA, or left untreated, and observed that DRAK2 and PKD comigrated as part of large molecular mass complexes (Fig. 5*C*). Treatment with PMA did not lead to a large difference in the stoichiometry of the complexes containing DRAK2. However, PMA significantly altered the size of complexes in which PKD migrated; we note that in response to PMA, activated PKD (phosphorylated on Ser^{916}) was then recruited to potentially the same complexes DRAK2 was contained within. We conclude in this study that DRAK2 interacts with PKD following activation of the latter kinase.

To understand where this interaction occurs within T cells, D10 cells were treated with thapsigargin, followed by subcellular fractionation to separate mitochondrial, nuclear, organelle-free cytosolic (S-100), and total plasma membrane (P-100) compartments. Thapsigargin-treated cells contained PKD in the nucleus, and multiple PKD isoforms were found in mitochondrial and plasma membrane fractions (Fig. 5*Di*, 5*Dii*), consistent with previous reports indicating that these are prominent sites of PKD translocation and activation, respectively (17). In accord with PKD's role in DRAK2 activation, we also found that activated DRAK2 was found at high levels in mitochondrial and plasma membrane fractions as well. Thus, whereas we are presently unclear about the substrates DRAK2 directly targets, these data suggest that the ability of DRAK2 to impact calcium signaling may originate from interactions taking place at mitochondria and/or plasma membranes. To gain further insight into where DRAK2 is localized during T cell activation, we used fluorescence microscopy and found that DRAK2 was indeed proximal to mitochondria, as visualized using MitoTracker Red and anti-DRAK2 mAbs. Although we found DRAK2 to be localized at or near mitochondria during resting conditions in some cells (Fig. 6*A*), its localization to mitochondria was enhanced upon treatment with thapsigargin (Fig. 6*B*). As

negative controls, staining of wild-type splenocytes with secondary Ab only, or staining of Drak2$^{-/-}$ cells with ant-DRAK2 plus secondary Abs both failed to demonstrate signal over background, indicating the specific detection of endogenous DRAK2 in vivo (Fig. 6*C*). Additionally, thapsigargin treatment led to strong induction of phospho-ERK staining, demonstrating that thapsigargin promotes various signaling cascades in these cells. Interestingly, we found that upon stimulation with thapsigargin, the DRAK2 signal formed much more prominent punctae, many of which could be seen within or proximal to areas of strong Mito-Tracker Red staining. These and the aforementioned results support the hypothesis that PKD and DRAK2 are recruited to high molecular mass complexes associated with mitochondria.

PKD phosphorylates DRAK2 in response to mitochondrial release of ROS

To determine whether PKD may regulate DRAK2 activity through direct phosphorylation, in vitro kinase assays were developed using recombinant isoforms of PKD2 and DRAK2. Because DRAK2 autophosphorylation might mask any signal that would result from transphosphorylation by PKD, kinase-dead DRAK2 (GST-DRAK2-K62A) was used as a potential in vitro PKD target (8, 32). As well, we used a C-terminal truncation mutant of DRAK2 (GST-DRAK2-ΔC) previously shown to lack in vitro kinase activity (8). Purification of GST-DRAK2-K62A yielded recombinant protein that migrated as a doublet by SDS-PAGE, and a cleavage product that is likely full-length DRAK2-K62A, as assessed by Coomassie staining (Fig. 7*A*). Kinase-dead DRAK2, as well as its cleavage product, and DRAK2-ΔC were subject to transphosphorylation upon incubation with active rPKD2 (Fig. 7*B*). Thus, we conclude that DRAK2 is a bona fide PKD target. We note that PKD was able to phosphorylate DRAK2 outside of its C terminus, suggesting that PKD-mediated phosphorylation occurs on a site in the 1–290 fragment of DRAK2. However, it is also quite possible that transphosphorylation events occur on its C terminus as well. We surmise that such transphosphorylation affects DRAK2 local structure, perhaps through phosphorylation of its activation loop present in the 1–290 fragment, a common means for kinase activation by other kinases (33).

PKD has been shown to be responsive to thapsigargin in a PLCγ-dependent manner, postulated to occur through positive feedback of calcium release on PLCγ activity (18), although the mechanism through which this occurs has been incompletely defined. Calcium is a known inducer of ROS, and ROS regulate PLCγ (34, 35). Because PKD has been well documented to respond to oxidative stress, we tested the hypothesis that PKD and DRAK2 respond to the generation of ROS following calcium-induced mitochondrial respiration. The ROS scavenger LNAC was effective in its ability to block both TCR cross-linking– and thapsigargin-induced DRAK2 activation (Fig. 8*A*–*C*), suggesting that ROS act as intermediates in the DRAK2 signaling cascade. LNAC potentially led to DRAK2 hyperphosphorylation, as seen by a shift in molecular mass (Fig. 8*B*). However, this phosphorylation could not be attributed to a specific pathway or due to increased autophosphorylation as no increase in phosphorylation on Ser^{12} was observed. Interestingly, the antioxidant BHA was also effective at blocking DRAK2 activity, but the superoxide dismutase (SOD)-mimetic MnTBAP was ineffectual (Fig. 8*C*). It should be noted that whereas LNAC and BHA work generally to directly scavenge ROS, the effect of MnTBAP is to convert these mitochondrial ROS into H_2O_2 (36), potentially affecting cellular signaling in a distinct manner.

As before, coexpression of CA-PKD and wild-type DRAK2 in 293T cells led to an increase in DRAK2 autophosphorylation (Fig. 8*D*). Importantly, phosphorylation of Ser^{12} in kinase-dead DRAK2 (K62A) was not influenced by CA-PKD, demonstrating that this autophosphorylation site is not itself a target of PKD. Whereas CA-PKD retains full activity in the presence of ROS scavengers, LNAC was partially effective in reducing Ser^{12}

phosphorylation on DRAK2, suggesting that this partial reduction in DRAK2 activity may have resulted from defective binding to PKD. Consistent with this, we observed that coimmunoprecipitation of PKD and DRAK2 from mitochondrial extracts was diminished by LNAC (Fig. 8*E*). These results demonstrate that mROS promote both PKD's activation and its oligomerization with DRAK2. To further demonstrate that mROS may be involved in DRAK2 activation, D10 T cells were treated with CCCP, an inhibitor of electron transport and mitochondrial respiraton. Under such conditions, uncoupling of electron transport by CCCP promotes the generation of mROS, which in turn activate PKD (17). This treatment alone led to DRAK2 activation, supporting the hypothesis that production of mROS is sufficient to induce mitochondrial DRAK2 activity (Fig. 8*F*), in accord with its ability to activate PKD.

Discussion

Regulation of calcium signaling during T cell activation is intimately linked with the decision to undergo apoptosis or a proliferative burst leading to the expansion of differentiated effector populations. This process is nonlinear in nature, and relies upon the amplification of proximal TCR events, such as tyrosine phosphorylation of the CD3 complex and PLCγ. ROS are potent regulators of tyrosine phosphatases that regulate proximal TCR events (37, 38). Recent work has demonstrated the direct effect of AgR-induced calcium mobilization on ROS production (34, 39). We show in this study that DRAK2 is a kinase that targets the influx of calcium following T cell activation. The kinase activity of DRAK2 is itself promoted by calcium entry following T cell activation, and dependent upon the subsequent generation of ROS, a byproduct of mitochondrial respiration. Because ROS may promote the amplification of receptor-mediated calcium entry, these studies have revealed how DRAK2 may be involved in a negative feedback loop that functions to limit this amplification process.

DRAK2 autophosphorylation on Ser^{12} has previously been demonstrated to correlate with its activation and is induced in response both to thapsigargin and anti-CD3 cross-linking (8). Importantly, the expression of DRAK2-S12A in Drak2-deficient T cells did not suppress calcium mobilization to a level comparable to reconstitution with wild-type DRAK2. Knockdown of DRAK2 in D10 T cells has recapitulated the Drak2-deficient phenotype (1, 2), demonstrating that increased calcium mobilization is a consequence of an acute lack of DRAK2 signaling, and is not due to a potential developmental defect in Drak2-deficient T cells. Whereas basal calcium levels and calcium released from intracellular stores were similar between knockdown and wild-type cells, extracellular calcium entry was greatly enhanced by diminished expression of DRAK2. Thus, we find that DRAK2 activation not only requires calcium entry through CRAC channels, but that DRAK2 serves to limit the amount of calcium influx upon activation.

ROS production is a direct consequence of increased calcium mobilization and has been documented to lead to PKD activation under certain cellular contexts (16, 17, 40–42). The finding that PKD is required for DRAK2 activation led us to ask whether calcium itself is sufficient for feedback inhibition by DRAK2, or whether oxidative stress may also play a role. Thapsigargin results in the depletion of ER-calcium stores and leads to calcium entry dependent on CRAC channel activity in T cells. Whereas blocking the effects of ROS with various scavengers may have an effect on AgR-induced calcium entry, ROS scavengers should not affect the ability of thapsigargin to promote extracellular calcium entry. Thus, we sought ROS scavengers with the ability to block both TCR cross-linking– and thapsigargin-induced DRAK2 activation, and found that LNAC and BHA could successfully block this, whereas the SOD-mimetic MnTBAP was ineffectual. Whereas the direct scavenging ability of LNAC and BHA may be sufficient to suppress DRAK2 activation, the enhanced

conversion of super-oxide anions to H_2O_2 by MnTBAP did not appear to be sufficient. Consistent with this, we failed to observe the induction of DRAK2 activity following treatment with H_2O_2 (data not shown). To substantiate the idea that mROS are required for DRAK2 activation, we employed a pharmacological agent to decouple electron transport, with resultant mROS production. Treatment with this drug alone was sufficient to promote PKD and DRAK2 activation, most likely at complexes assembled at or near mitochondria. To our knowledge, these are the first results to demonstrate a distinct subcellular compartment in which DRAK2 is activated, and suggest that DRAK2 may serve to regulate not only calcium homeostasis, but also to act in the response to oxidative stress. The latter hypothesis is supported by the observation of increased ROS levels in Drak2$^{-/-}$ T cells following stimulation with the super-antigen staphylococcal enterotoxin B (SEB) (3).

Recent work with PKD has shown that PKD localizes to mitochondria in response to oxidative stress, and that 1,2-diac-ylglycerol produced on mitochondrial membranes is responsible for this translocation (43). To substantiate the idea that DRAK2 responds to mROS-induced PKD, we used subcellular fractionation to determine where activated DRAK2 is found in T cells. DRAK2 autophosphorylation was prominently detected in mitochondrial fractions, fractions that also contained a substantial amount of activated PKD. This hypothesis was supported by fluorescence microscopic imaging of endogenous DRAK2, in which treatment with thapsigargin resulted in the accumulation of punctae that colocalized with MitoTracker Red-stained mitochondria. Whereas treatment with PMA did not significantly alter the stoichiometry of putative DRAK2 complexes shown by blue-native PAGE, it led to the enhanced recruitment of an activated PKD isoform to comigrating DRAK2 complexes. This is in accord with coimmunoprecipitation data showing that DRAK2 interacts with PKD upon treatment with PMA or thapsigargin, but not under resting conditions, and that coimmunoprecipitation of DRAK2 with anti-PKD could be observed in mitochondrial fractions, but not using whole-cell lysates. Together with results showing that selective ROS scavengers blocked DRAK2 activation and coimmunoprecipitation with PKD, and that this activation can be achieved independently through disruption of mitochondrial electron transport, we favor the hypothesis that DRAK2 is activated at or near mitochondria in a manner dependent on mROS-induced PKD.

To gain insight into the mechanism by which PKD is required for DRAK2 activation, rDRAK2 was subjected to in vitro kinase assays with active rPKD. Kinase-dead DRAK2, as well as a C-terminal truncation mutant that also lacks autocatalytic activity, were phosphorylated by PKD in vitro, suggesting that PKD and DRAK2 colocalization results in transphosphorylation of DRAK2 by PKD, in turn leading to DRAK2 activation. PKCδ has recently been shown to phosphorylate DRAK2 on Ser^{351} following exposure of a rat colon carcinoma cell line to UV irradiation, leading to its nuclear translocalization (7). Given that PKD phosphorylates an isoform of DRAK2 lacking its 80-aa C-terminal domain, these findings support the notion that PKCδ and PKD act distinctly in regulating DRAK2. Further supporting this hypothesis, the sub-cellular fractionation results reported in this work demonstrate that autocatalytic DRAK2 activity is found in mitochondrial, but not nuclear or cytosolic fractions. Thus, it may be that DRAK2 serves several purposes in cells, and that regulation of its sub-cellular trafficking, perhaps through differential phosphorylation, may be key to distinguishing such functions.

There are several key pieces of evidence suggesting that ROS production plays a crucial role in T cell function and survival. A reciprocal relationship between ROS and Bcl-2 levels within cells has been demonstrated (44), and work in T cells has demonstrated that ROS sensitize T cells to apoptosis through downregulation of Bcl-2 (36). Drak2$^{-/-}$ cells exhibit lower levels of Bcl-x_L following stimulation with SEB, which contributes to their defect in survival, as restoration of Bcl-x_L levels rescues this defect (3). Drak2$^{-/-}$ cells as well

display increased levels of cellular ROS following stimulation with SEB, and it is possible that the observed downregulation of Bcl-x_L depends on this in these cells. Control over the strength of AgR signaling has been shown to rely in part on a calcium-oxidant loop and has identified protein tyrosine phosphatases and ROS-generating enzymes as key molecular targets that positively feed back on proximal TCR events (45). It is likely that the increased levels of ROS observed in DRAK2$^{-/-}$ cells are a direct result of increased calcium mobilization due to the absence of DRAK2. Recent work in B cells has shown that ROS production following B cell activation likewise plays an important role in cellular metabolism (38). BCR-mediated ROS production was shown to be required for sustained activation of Syk and Akt, and disruption of this led to defective mitochondrial respiration and glycolytic rates, resulting in impaired proliferation. In addition, control over mitochondrial calcium uptake has been shown to be critical for regulation of mitochondrial respiration and maintenance of cellular homeostasis (46). The finding that DRAK2 activity is tightly linked with cellular levels of calcium, and that DRAK2 is highly catalytic at mitochondria supports the notion that DRAK2 may be involved in the direct regulation of mitochondrial bio-energetics and requires further investigation. Recent work on immune synapses has revealed an important role for mitochondria in regulating calcium influx, and that mitochondrial uptake of calcium during T cell activation is critical in this process (47, 48). Our work in this study suggests that tight regulation of calcium entry impacts T cell activation and subsequent ROS production most likely through a PKD-DRAK2 signaling axis, and is a critical process with direct consequences on the effectiveness of an immune response. Although we observe acute effects of DRAK2 signaling upon T cell activation, it will be important to determine whether DRAK2 serves alternative functions at different stages following activation, and whether DRAK2 impacts calcium homeostasis and survival via parallel or serial pathways.

In conclusion, we provide evidence that PKD is required for DRAK2 to exert control over calcium mobilization upon T cell activation. This process is shown in this work to require not only the influx of extracellular calcium, but also the production of mROS, both of which occur soon after AgR stimulation of lymphocytes (49, 50). Furthermore, DRAK2 activation occurs at mitochondria, and most likely involves colocalization of active PKD to mitochondria, followed by transphosphorylation of DRAK2 that promotes its catalytic activity. Taken together, DRAK2 and PKD are described to constitute a signaling axis that serves to maintain calcium homeostasis and limit the generation of ROS following T cell AgR signaling. It has been established that mice lacking DRAK2 are resistant to organ-specific autoimmune disease models, including experimental autoimmune encephalomyelitis and type I diabetes, yet possess normal responses to viral infection (1, 3, 4, 51). Although hyperresponsive to weak antigenic stimuli, T cells lacking DRAK2 fail to survive in selective settings. Thus, a greater understanding of how DRAK2 controls calcium homeostasis and impacts the response to oxidative stress will likely provide important concepts for selective control of T cell responses.

Acknowledgments

This work was supported by the National Insititutes of Health (AI63419 to C.M.W.; NS14609 to M.D.C.); the Arthritis National Research Foundation (to C.M.W.); the National Multiple Sclerosis Society (to C.M.W.); and the Juvenile Diabetes Research Foundation (to C.M.W.). R.H.N. was supported by National Institutes of Health Immunology Research Training Grant T32 AI-060573.

We thank Drs. E. Rozengurt, A. Toker, B. Wen, and D. Cantrell for reagents. We also thank Dr. Naomi Morrissettte for assistance with microscopy and Drs. David Fruman and Aimee Edinger for helpful comments regarding this manuscript.

Abbreviations in this article

BHA	butylated hydroxyanisole
$[Ca^{2+}]_i$	intracellular calcium concentration
CA-PKD	constitutively active protein kinase D mutant
CCCP	carbonyl cyanide *m*-chloro phenyl hydrazone
CRAC	Ca^{2+} release-activated Ca^{2+} channel
DAPK	death-associated protein kinase
ER	endoplasmic reticulum
IP	immunoprecipitation
IP_3	inositol 1,4,5-triphosphate
LNAC	*N*-acetyl-L-cysteine
MBP	myelin basic protein
MLC	myosin L chain
MnTBAP	Mn (III) tetrakis (4-benzoic acid) porphyrin
mROS	mitochondria-derived reactive oxygen species
PKC	protein kinase C
PKD	protein kinase D
PLCγ	phospholipase Cγ
ROS	reactive oxygen species
SEB	staphylococcal enterotoxin B
SOCE	store-operated capacitative calcium entry
SOD	superoxide dismutase

References

1. McGargill MA, Wen BG, Walsh CM, Hedrick SM. A deficiency in Drak2 results in a T cell hypersensitivity and an unexpected resistance to autoimmunity. Immunity. 2004; 21:781–791. [PubMed: 15589167]
2. Friedrich ML, Wen BG, Bain G, Kee BL, Katayama C, Murre C, Hedrick SM, Walsh CM. DRAK2, a lymphoid-enriched DAP kinase, regulates the TCR activation threshold during thymocyte selection. Int Immunol. 2005; 17:1379–1390. [PubMed: 16172133]
3. Ramos SJ, Hernandez JB, Gatzka M, Walsh CM. Enhanced T cell apoptosis within Drak2-deficient mice promotes resistance to autoimmunity. J Immunol. 2008; 181:7606–7616. [PubMed: 19017949]
4. McGargill MA, Choy C, Wen BG, Hedrick SM. Drak2 regulates the survival of activated T cells and is required for organ-specific autoimmune disease. J Immunol. 2008; 181:7593–7605. [PubMed: 19017948]
5. Kögel D, Prehn JH, Scheidtmann KH. The DAP kinase family of pro-apoptotic proteins: novel players in the apoptotic game. Bioessays. 2001; 23:352–358. [PubMed: 11268041]
6. Kuwahara H, Nakamura N, Kanazawa H. Nuclear localization of the serine/threonine kinase DRAK2 is involved in UV-induced apoptosis. Biol Pharm Bull. 2006; 29:225–233. [PubMed: 16462023]
7. Kuwahara H, Nishizaki M, Kanazawa H. Nuclear localization signal and phosphorylation of serine350 specify intracellular localization of DRAK2. J Biochem. 2008; 143:349–358. [PubMed: 18084041]

8. Friedrich ML, Cui M, Hernandez JB, Weist BM, Andersen HM, Zhang X, Huang L, Walsh CM. Modulation of DRAK2 autophosphorylation by antigen receptor signaling in primary lymphocytes. J Biol Chem. 2007; 282:4573–4584. [PubMed: 17182616]
9. Rozengurt E, Rey O, Waldron RT. Protein kinase D signaling. J Biol Chem. 2005; 280:13205–13208. [PubMed: 15701647]
10. Irie A, Harada K, Tsukamoto H, Kim JR, Araki N, Nishimura Y. Protein kinase D2 contributes to either IL-2 promoter regulation or induction of cell death upon TCR stimulation depending on its activity in Jurkat cells. Int Immunol. 2006; 18:1737–1747. [PubMed: 17077180]
11. Matthews SA, Rozengurt E, Cantrell D. Protein kinase D: a selective target for antigen receptors and a downstream target for protein kinase C in lymphocytes. J Exp Med. 2000; 191:2075–2082. [PubMed: 10859332]
12. Marklund U, Lightfoot K, Cantrell D. Intracellular location and cell context-dependent function of protein kinase D. Immunity. 2003; 19:491–501. [PubMed: 14563314]
13. Matthews SA, Iglesias T, Rozengurt E, Cantrell D. Spatial and temporal regulation of protein kinase D (PKD). EMBO J. 2000; 19:2935–2945. [PubMed: 10856238]
14. Waldron RT, Rozengurt E. Protein kinase C phosphorylates protein kinase D activation loop Ser744 and Ser748 and releases autoinhibition by the pleckstrin homology domain. J Biol Chem. 2003; 278:154–163. [PubMed: 12407104]
15. Sinnett-Smith J, Jacamo R, Kui R, Wang YM, Young SH, Rey O, Waldron RT, Rozengurt E. Protein kinase D mediates mitogenic signaling by Gq-coupled receptors through protein kinase C-independent regulation of activation loop Ser744 and Ser748 phosphorylation. J Biol Chem. 2009; 284:13434–13445. [PubMed: 19289471]
16. Zhang W, Zheng S, Storz P, Min W. Protein kinase D specifically mediates apoptosis signal-regulating kinase 1-JNK signaling induced by H2O2 but not tumor necrosis factor. J Biol Chem. 2005; 280:19036–19044. [PubMed: 15755722]
17. Storz P, Döppler H, Toker A. Protein kinase D mediates mitochondrion-to-nucleus signaling and detoxification from mitochondrial reactive oxygen species. Mol Cell Biol. 2005; 25:8520–8530. [PubMed: 16166634]
18. Kunkel MT, Toker A, Tsien RY, Newton AC. Calcium-dependent regulation of protein kinase D revealed by a genetically encoded kinase activity reporter. J Biol Chem. 2007; 282:6733–6742. [PubMed: 17189263]
19. Koncz P, Szanda G, Fülöp L, Rajki A, Spät A. Mitochondrial Ca2+ uptake is inhibited by a concerted action of p38 MAPK and protein kinase D. Cell Calcium. 2009; 46:122–129. [PubMed: 19631981]
20. Cahalan MD, Chandy KG. The functional network of ion channels in T lymphocytes. Immunol Rev. 2009; 231:59–87. [PubMed: 19754890]
21. Crabtree GR, Olson EN. NFAT signaling: choreographing the social lives of cells. Cell. 2002; 109:S67–S79. [PubMed: 11983154]
22. Dower NA, Stang SL, Bottorff DA, Ebinu JO, Dickie P, Ostergaard HL, Stone JC. RasGRP is essential for mouse thymocyte differentiation and TCR signaling. Nat Immunol. 2000; 1:317–321. [PubMed: 11017103]
23. Altman A, Isakov N, Baier G. Protein kinase Ctheta: a new essential superstar on the T-cell stage. Immunol Today. 2000; 21:567–573. [PubMed: 11094261]
24. Feske S. Calcium signalling in lymphocyte activation and disease. Nat Rev Immunol. 2007; 7:690–702. [PubMed: 17703229]
25. Gwack Y, Feske S, Srikanth S, Hogan PG, Rao A. Signalling to transcription: store-operated Ca2+ entry and NFAT activation in lymphocytes. Cell Calcium. 2007; 42:145–156. [PubMed: 17572487]
26. Gatzka M, Newton RH, Walsh CM. Altered thymic selection and increased autoimmunity caused by ectopic expression of DRAK2 during T cell development. J Immunol. 2009; 183:285–297. [PubMed: 19542440]
27. Gschwendt M, Dieterich S, Rennecke J, Kittstein W, Mueller HJ, Johannes FJ. Inhibition of protein kinase C mu by various inhibitors: differentiation from protein kinase C isoenzymes. FEBS Lett. 1996; 392:77–80. [PubMed: 8772178]

28. Kaye J, Porcelli S, Tite J, Jones B, Janeway CA Jr. Both a monoclonal antibody and antisera specific for determinants unique to individual cloned helper T cell lines can substitute for antigen and antigen-presenting cells in the activation of T cells. J Exp Med. 1983; 158:836–856. [PubMed: 6193236]
29. Kerschbaum HH, Cahalan MD. Single-channel recording of a store-operated Ca2+ channel in Jurkat T lymphocytes. Science. 1999; 283:836–839. [PubMed: 9933165]
30. Cahalan MD. STIMulating store-operated Ca(2+) entry. Nat Cell Biol. 2009; 11:669–677. [PubMed: 19488056]
31. Gwack Y, Srikanth S, Oh-Hora M, Hogan PG, Lamperti ED, Yamashita M, Gelinas C, Neems DS, Sasaki Y, Feske S, et al. Hair loss and defective T- and B-cell function in mice lacking ORAI1. Mol Cell Biol. 2008; 28:5209–5222. [PubMed: 18591248]
32. Sanjo H, Kawai T, Akira S. DRAKs, novel serine/threonine kinases related to death-associated protein kinase that trigger apoptosis. J Biol Chem. 1998; 273:29066–29071. [PubMed: 9786912]
33. Nolen B, Taylor S, Ghosh G. Regulation of protein kinases; controlling activity through activation segment conformation. Mol Cell. 2004; 15:661–675. [PubMed: 15350212]
34. Singh DK, Kumar D, Siddiqui Z, Basu SK, Kumar V, Rao KV. The strength of receptor signaling is centrally controlled through a cooperative loop between Ca2+ and an oxidant signal. Cell. 2005; 121:281–293. [PubMed: 15851034]
35. Lee K, Esselman WJ. Inhibition of PTPs by H(2)O(2) regulates the activation of distinct MAPK pathways. Free Radic Biol Med. 2002; 33:1121–1132. [PubMed: 12374624]
36. Hildeman DA, Mitchell T, Teague TK, Henson P, Day BJ, Kappler J, Marrack PC. Reactive oxygen species regulate activation-induced T cell apoptosis. Immunity. 1999; 10:735–744. [PubMed: 10403648]
37. Tonks NK. Redox redux: revisiting PTPs and the control of cell signaling. Cell. 2005; 121:667–670. [PubMed: 15935753]
38. Reth M. Hydrogen peroxide as second messenger in lymphocyte activation. Nat Immunol. 2002; 3:1129–1134. [PubMed: 12447370]
39. Capasso M, Bhamrah MK, Henley T, Boyd RS, Langlais C, Cain K, Dinsdale D, Pulford K, Khan M, Musset B, et al. HVCN1 modulates BCR signal strength via regulation of BCR-dependent generation of reactive oxygen species. Nat Immunol. 2010; 11:265–272. [PubMed: 20139987]
40. Döppler H, Storz P. A novel tyrosine phosphorylation site in protein kinase D contributes to oxidative stress-mediated activation. J Biol Chem. 2007; 282:31873–31881. [PubMed: 17804414]
41. Waldron RT, Rozengurt E. Oxidative stress induces protein kinase D activation in intact cells: involvement of Src and dependence on protein kinase C. J Biol Chem. 2000; 275:17114–17121. [PubMed: 10748111]
42. Eisenberg-Lerner A, Kimchi A. DAP kinase regulates JNK signaling by binding and activating protein kinase D under oxidative stress. Cell Death Differ. 2007; 14:1908–1915. [PubMed: 17703233]
43. Cowell CF, Döppler H, Yan IK, Hausser A, Umezawa Y, Storz P. Mitochondrial diacylglycerol initiates protein-kinase D1-mediated ROS signaling. J Cell Sci. 2009; 122:919–928. [PubMed: 19258390]
44. Chang WK, Yang KD, Chuang H, Jan JT, Shaio MF. Glutamine protects activated human T cells from apoptosis by up-regulating glutathione and Bcl-2 levels. Clin Immunol. 2002; 104:151–160. [PubMed: 12165276]
45. Williams MS, Kwon J. T cell receptor stimulation, reactive oxygen species, and cell signaling. Free Radic Biol Med. 2004; 37:1144–1151. [PubMed: 15451054]
46. Cárdenas C, Miller RA, Smith I, Bui T, Molgó J, Müller M, Vais H, Cheung KH, Yang J, Parker I, et al. Essential regulation of cell bio-energetics by constitutive InsP3 receptor Ca2+ transfer to mitochondria. Cell. 2010; 142:270–283. [PubMed: 20655468]
47. Hoth M, Fanger CM, Lewis RS. Mitochondrial regulation of store-operated calcium signaling in T lymphocytes. J Cell Biol. 1997; 137:633–648. [PubMed: 9151670]
48. Quintana A, Schwindling C, Wenning AS, Becherer U, Rettig J, Schwarz EC, Hoth M. T cell activation requires mitochondrial translocation to the immunological synapse. Proc Natl Acad Sci USA. 2007; 104:14418–14423. [PubMed: 17726106]

49. Jones RG, Bui T, White C, Madesh M, Krawczyk CM, Lindsten T, Hawkins BJ, Kubek S, Frauwirth KA, Wang YL, et al. The proapoptotic factors Bax and Bak regulate T cell proliferation through control of endoplasmic reticulum Ca(2+) homeostasis. Immunity. 2007; 27:268–280. [PubMed: 17692540]

50. Jones RG, Thompson CB. Revving the engine: signal transduction fuels T cell activation. Immunity. 2007; 27:173–178. [PubMed: 17723208]

51. Ramos SJ, Hardison JL, Stiles LN, Lane TE, Walsh CM. Anti-viral effector T cell responses and trafficking are not dependent upon DRAK2 signaling following viral infection of the central nervous system. Autoimmunity. 2007; 40:54–65. [PubMed: 17364498]

52. Kerschbaum HH, Negulescu PA, Cahalan MD. Ion channels, Ca2+ signaling, and reporter gene expression in antigen-specific mouse T cells. J Immunol. 1997; 159:1628–1638. [PubMed: 9257822]

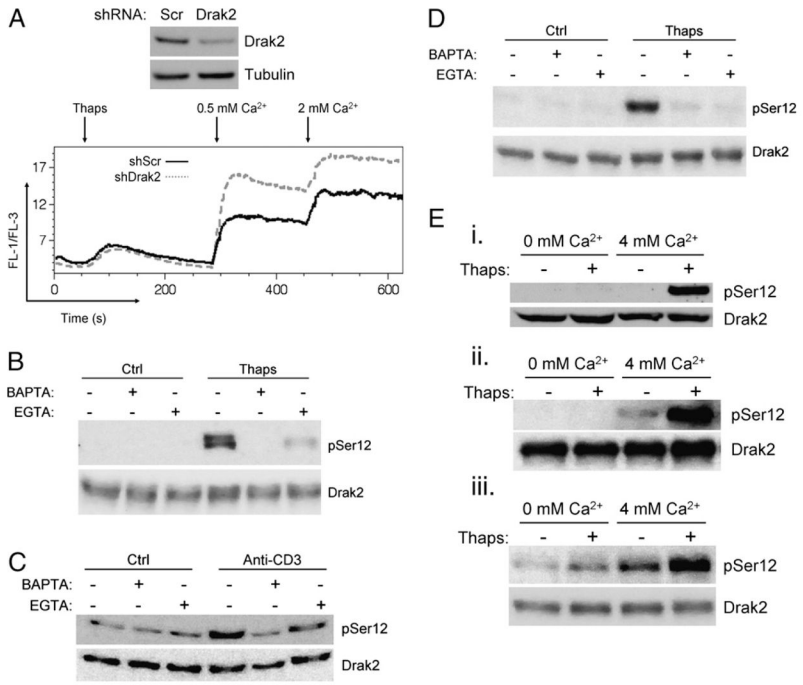

FIGURE 1.

DRAK2 activity requires and negatively impacts SOCE. *A*, Enhanced calcium mobilization in DRAK2-knockdown D10 T cells. D10 T cells were infected with retrovirus expressing a short hairpin targeting DRAK2, or a nonspecific short hairpin. Cells were loaded with the calcium indicator dyes Fura red and Fluo-3, and changes in $[Ca^{2+}]_i$ were measured by flow cytometry in response to 1 μM thapsigargin, administered to cells in media without calcium, followed by addition of 0.5 mM $CaCl_2$ and then 2 mM $CaCl_2$. *B*, Thapsigargin-induced DRAK2 activation is blocked by BAPTA-AM and EGTA. D10 T cells were preincubated with 40 μM BAPTA-AM or 4 mM EGTA, and then treated with 1 μM thapsigargin or DMSO for 5 min, followed by lysis and Western blotting with Abs to DRAK2 and DRAK2 phosphorylated on Ser^{12} (pSer12). *C*, Anti-CD3 cross-linking–induced DRAK2 activation is blocked by BAPTA-AM and EGTA. D10 T cells were preincubated with 40 μM BAPTA-AM or 4 mM EGTA, and then treated with 5 μg/ml 2C11-biotin for 2 min, followed by 40 μg/ml streptavidin for 5 min. Lysate was subjected to SDS-PAGE and probed with the indicated Abs. *D*, BAPTA-AM and EGTA block DRAK2 activation in thymocytes. Thymocytes were stimulated as in *B*. *E*, Extracellular calcium is required for DRAK2 activation to occur. Jurkat T cells (*i*), thymocytes (*ii*), and D10 T cells (*iii*) were incubated in HBSS with or without calcium, and treated with 1 mM thapsigargin, or DMSO, for 5 min, followed by lysis and Western blotting.

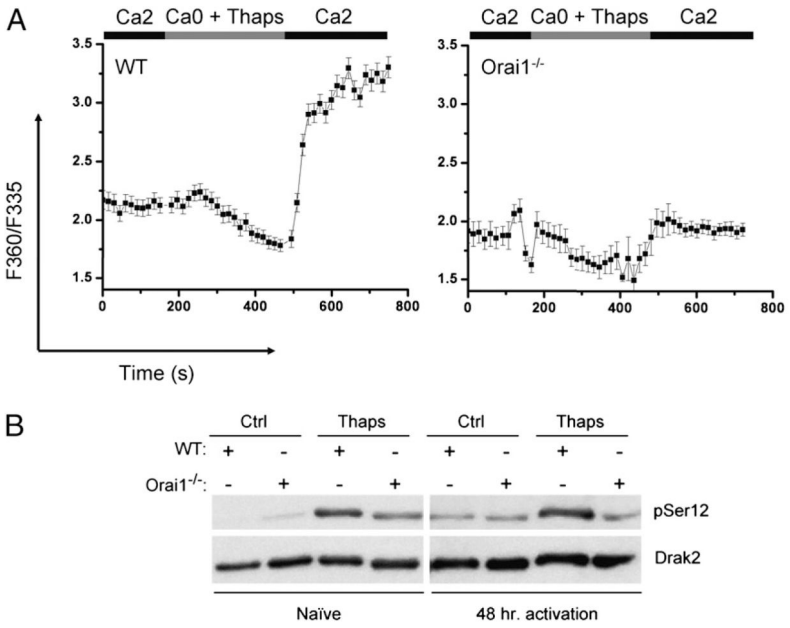

FIGURE 2.

Orai1, an essential component of the CRAC channel, is necessary for DRAK2 activity. *A*, Orai1-deficient T cells have defect in calcium entry. Negatively selected wild-type and *Orai1*$^{-/-}$ T cells were activated for 48 h in plates coated with 0.5 μg anti-CD3 cross-linked with anti-hamster Abs, in the presence of 0.2 μg/ml anti-CD28. Cells were then loaded with 2 mM fura 2-AM, and variation of $[Ca^{2+}]_i$ was monitored by single-cell imaging (52). ER calcium stock was released with 1 μM thapsigargin for 5 min in calcium-free media (Ca0 + Thaps), and the CRAC-dependent calcium uptake was induced by addition of 2 mM Ca^{2+} (Ca2) in the perfused media. *B*, DRAK2 activation is slightly impaired in naive Orai1-deficient T cells, and severely impaired in activated Orai1-deficient T cells. Naive and 48-h–activated wild-type and *Orai1*$^{-/-}$ purified T cells were treated with thapsigargin or DMSO for 5 min, and lysates were subjected to SDS-PAGE and probed with the indicated Abs.

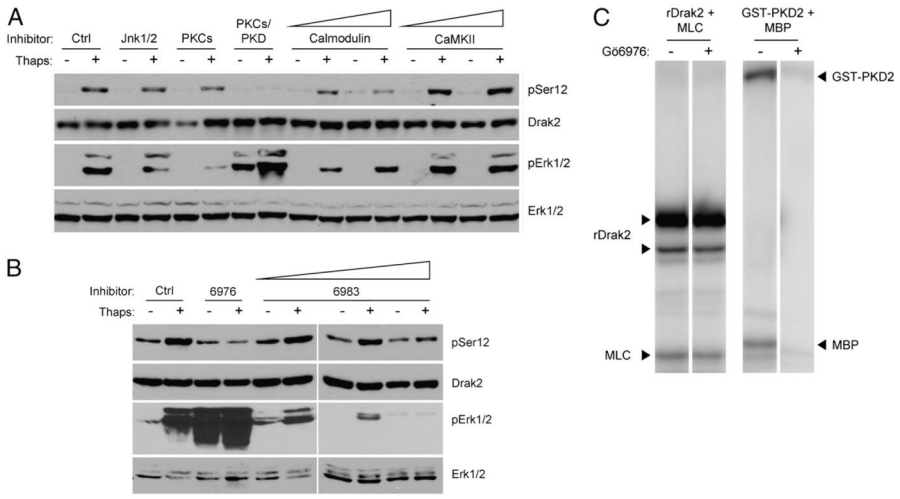

FIGURE 3.

Blockade of DRAK2 activity by the PKD inhibitor Gö6976. *A*, A screen of inhibitors targeting thapsigargin-induced pathways identifies Gö6976 as a potent blocker of DRAK2 activity. D10 T cells were preincubated with DMSO, 1 μM SP-600125 (JNK1/2 inhibitor), 1 μM Ro-31-8425 (classical PKC inhibitor), 1 μM Gö6976 (PKC/PKD inhibitor), 10 and 30 μM fluphenazine (calmodulin inhibitor), or 40 and 60 μM KN-93 (CaMKII inhibitor) for 30 min, followed by treatment with 1 μM thapsigargin or DMSO for 5 min. Lysates were subjected to SDS-PAGE and probed with the indicated Abs. *B*, PKC isoforms are not involved in DRAK2 activation. D10 T cells were preincubated with DMSO, 1 μM Gö6976, or 1, 10, and 30 μM Gö6983 for 30 min, followed by treatment with 1 μM thapsigargin or DMSO for 5 min. Lysates were subjected to SDS-PAGE and probed with the indicated Abs. *C*, Gö6976 effectively blocks the T cell relevant PKD2 isoform, but is ineffective at blocking DRAK2 catalytic activity directly. In vitro kinase assay of recombinant DRAK2 or GST-PKD2 with MLC or MBP as transphosphorylation targets, respectively, in the presence or absence of 2 μM Gö6976.

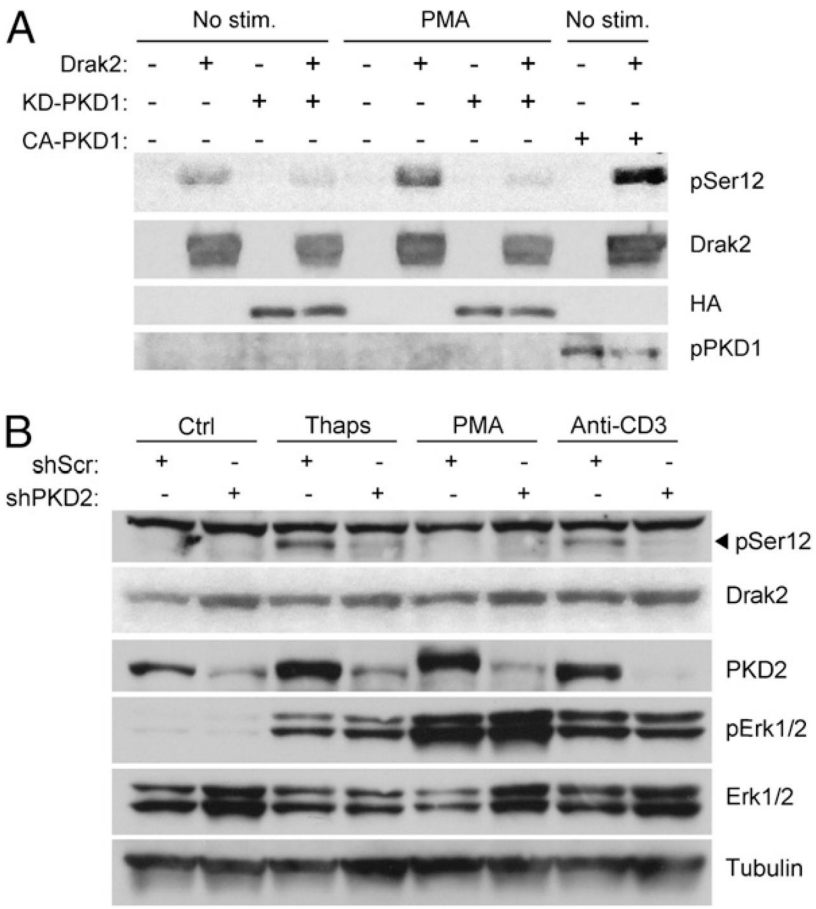

FIGURE 4.

PKD is required for DRAK2 activation. *A*, A kinase-dead PKD1 mutant reduces basal and PMA-induced levels of DRAK2 autophosphorylation, whereas CA-PKD1 enhances basal levels of DRAK2 autophosphorylation. The 293T cells were transfected with pEGFP or pEGFP-DRAK2, plus pcDNA3, pcDNA3-HA-PKD1-K612W (kinase-dead mutant [KD-PKD1]), or pEGFP-PKD1-S738/742E (CA-PKD1). Twenty-four hours later, transfected cells were treated with PMA (200 ng/ml) or DMSO for 10 min, lysed, and probed with the indicated Abs. Anti-PKD1 Ser^{916} was used for p-PKD. *B*, PKD2 knockdown in Jurkat T cells blocks thapsigargin- and anti-CD3 cross-linking–induced DRAK2 activation. pSM2c-shScrambled (shScr) or pSM2c-shPKD2 (shPKD2) expressing retroviruses were used to infect Jurkat T cells. Following infection, selection with puromycin was maintained for 2 d, followed by stimulation with 1 mM thapsigargin, 200 ng/ml PMA, and 5 μg/ml 2C11-biotin cross-linked with 40 μg/ml streptavidin for 5 min. Lysates were resolved by SDS-PAGE and probed with the indicated Abs.

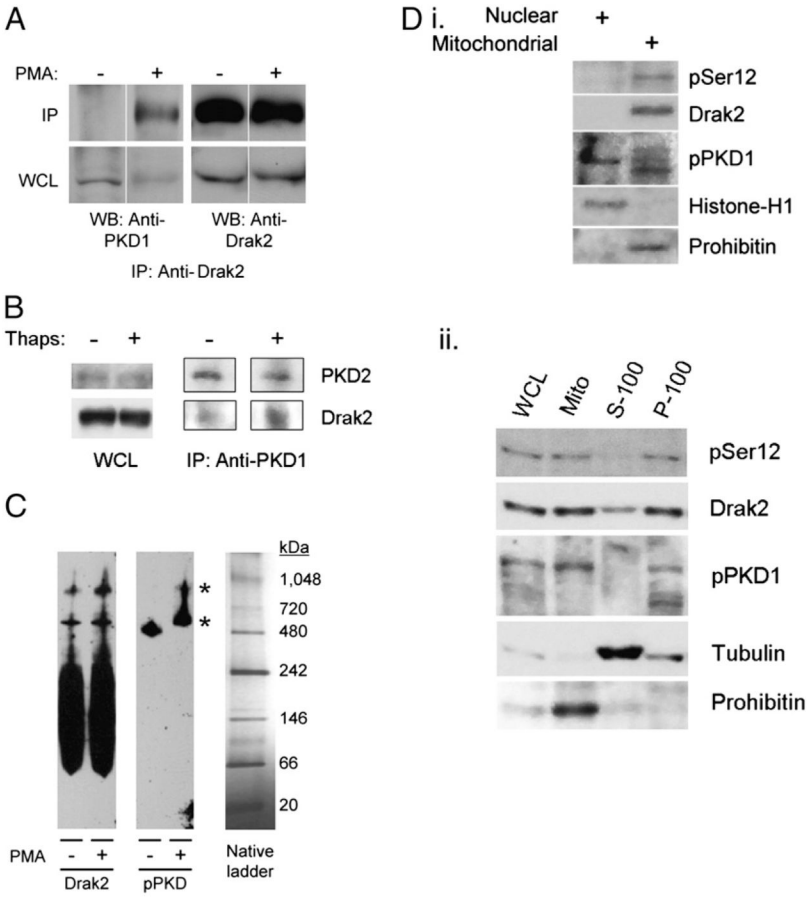

FIGURE 5.

DRAK2 interacts with activated PKD at the mitochondria. *A*, Endogenous DRAK2 and PKD coimmunoprecipitate in response to PMA treatment in D10 T cells. D10 T cells were treated with 200 ng/ml PMA, or with DMSO, for 5 min, followed by lysis in IP buffer and immunoprecipitation using anti-DRAK2 mAbs. Immunoprecipitates were subjected to SDS-PAGE and probed with the indicated Abs. *B*, Anti-PKD coimmunoprecipitates DRAK2. DRAK2-transgenic thymocytes were treated with 1 μM thapsigargin, or with DMSO, for 5 min, followed by lysis in IP buffer and immunoprecipitation using an anti-PKD1 Ab. *C*, DRAK2 comigrates with an active PKD isoform as part of two distinct high-m.w. complexes. D10 T cells were treated with 200 ng/ml PMA or DMSO for 5 min, lysed in blue-native PAGE lysis buffer (Invitrogen), and subjected to blue-native PAGE, followed by Western blotting, and probed with the indicated Abs. Asterisks mark complexes in which DRAK2 and phospho-PKD comigrate. Anti-PKD1 Ser^{916} was used for p-PKD. *D*, Autophosphorylated DRAK2 and activated PKD colocalize to mitochondria in D10 T cells. D10 T cells were treated with 1 μM thapsigargin, and lysate was fractionated into nuclear, mitochondrial, organelle-free cytosolic (S-100), and plasma membrane (P-100) fractions by differential centrifugation. Fractions were subjected to SDS-PAGE and probed with the indicated Abs. Anti-PKD1 $Ser^{744/748}$ was used for p-PKD.

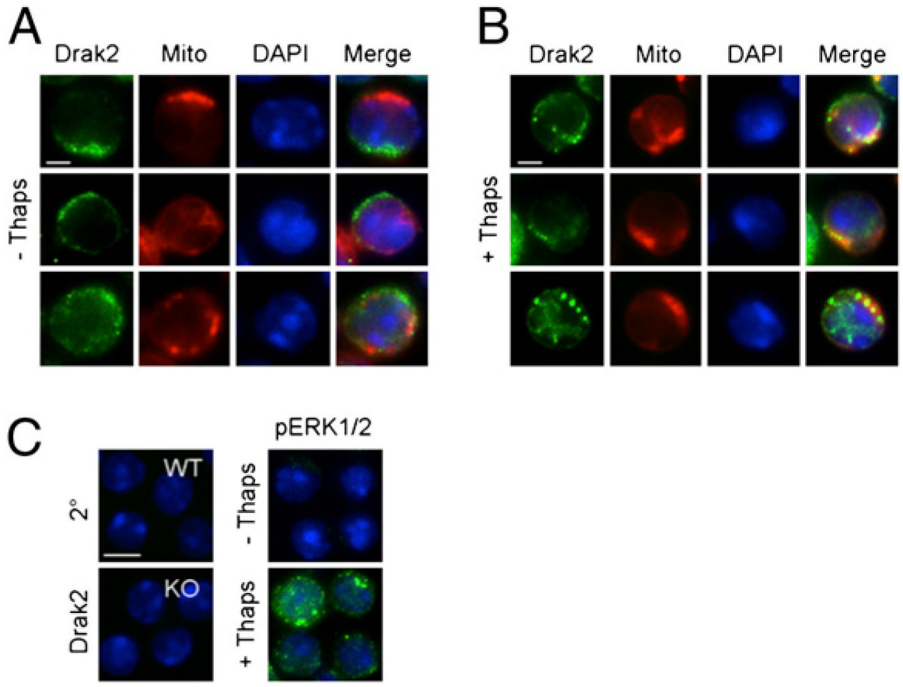

FIGURE 6.

Immunofluorescence images of DRAK2 and mitochondrial colocalization. Whole splenocytes were stained with MitoTracker Red, adhered to poly(L-lysine)-coated coverslips, stimulated with vehicle (0.1% v/v DMSO) (*A*) or with 1 μM thapsigargin (*B*) for 5 min, fixed, permeabilized, and stained with anti-DRAK2, followed by incubation with anti-rabbit Alexa Fluor 488, and mounted with medium containing DAPI. *C*, Control images of wild-type splenocytes stained with secondary only (as used in *A* and *B*), DRAK2$^{-/-}$ (knockout [KO]) cells stained as in *A* and *B*, and wild-type cells stimulated as in *A* and *B*, using anti-pERK1/2 as primary Ab to visualize activation.

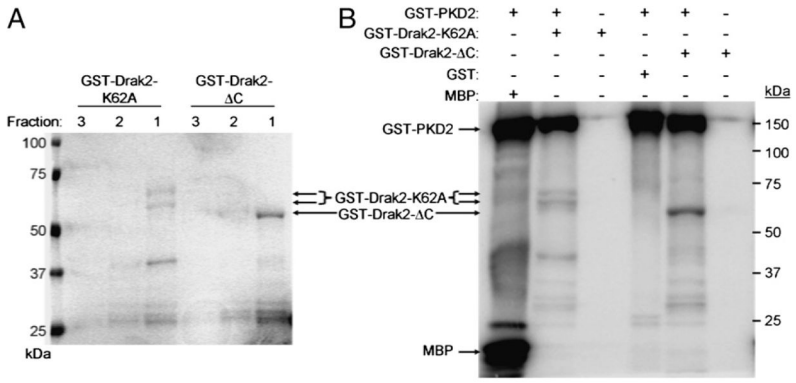

FIGURE 7.

DRAK2 is a direct phosphorylation target of PKD. *A*, Purified rGST-kinase–dead DRAK2 (K62A) and a GST-DRAK2 C-terminal truncation mutant (ΔC) migration in SDS-PAGE. Eluted GST proteins were resolved by SDS-PAGE, followed by Coomassie staining. A total of 20 μl of each 500-μl fraction was loaded. *B*, PKD phosphorylates DRAK2 in vitro on at least one residue outside of its C-terminal domain. A total of 200 ng purified GST-PKD2 was subjected to an in vitro kinase assay with 5 μg MBP as a positive control for transphosphorylation, 5 μg GST-DRAK2-K62A, 5 μg GST-DRAK2-ΔC, or 5 μg GST. The same amount of GST-DRAK2-K62A and GST-DRAK2-ΔC was subjected to in vitro kinase assays without GST-PKD2 as control.

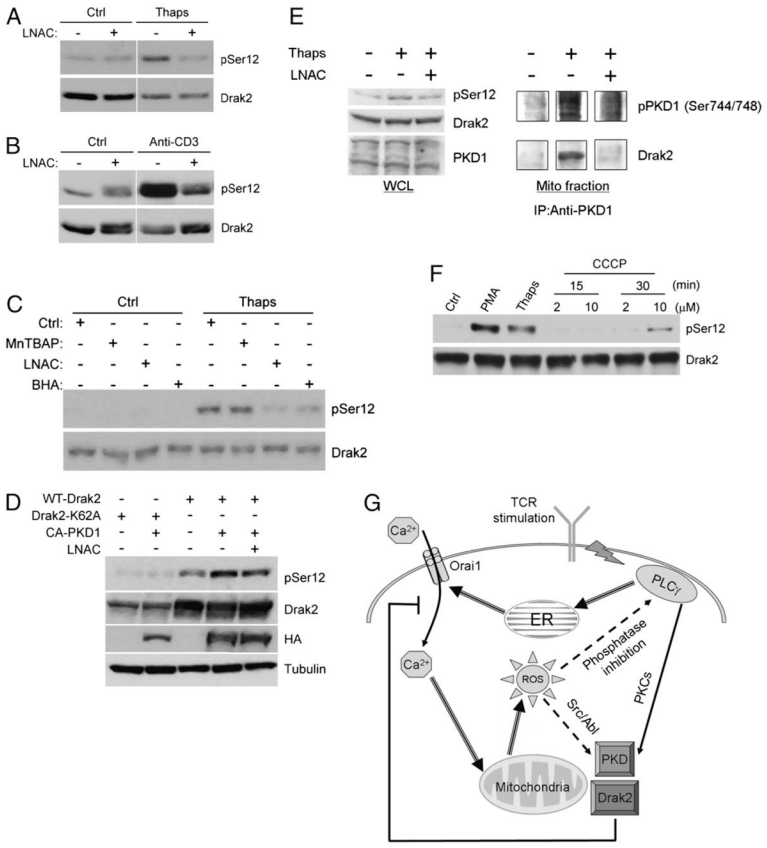

FIGURE 8.

DRAK2 intersects with the PKD pathway through ROS. *A*, The ROS scavenger LNAC blocks anti-CD3 cross-linking–induced DRAK2 activation. D10 T cells were preincubated with 12 mM LNAC for 30 min prior to stimulation with 5 μg/ml 2C11-biotin cross-linked with 40 μg/ml streptavidin for 5 min. Lysates were resolved by SDS-PAGE and probed with the indicated Abs. *B*, The ROS scavenger LNAC blocks thapsigargin-induced DRAK2 activation. D10 T cells were preincubated with 12 mM LNAC for 30 min prior to stimulation with 1 μM thapsigargin or DMSO, for 5 min. Lysates were resolved by SDS-PAGE and probed with the indicated Abs. *C*, LNAC and the antioxidant BHA block DRAK2 activation, whereas the SOD-mimetic, MnTBAP, is ineffective at blocking DRAK2 activation. Thymocytes were preincubated with 150 μM MnTBAP, 12 mM LNAC, or 100 μM BHA for 30 min prior to stimulation with 1 μM thapsigargin or DMSO for 5 min. Lysates were resolved by SDS-PAGE and probed with the indicated Abs. *D*, Kinase-dead DRAK2 does not autophosphorylate on Ser^{12}, and LNAC partially blocks induction of phosphor-Ser^{12} on WT-DRAK2 in the presence of CA-PKD1. The 293T cells were transfected with pEGFP-DRAK2 or pEGFP-DRAK2-K62A in combination with pcDNA3.1 or pEGFP-PKD1-S738/742E (CA-PKD1). Thirty minutes before lysis, cells were left untreated or treated with 12 mM LNAC. *E*, LNAC blocks DRAK2 and PKD coimmunoprecipitation. Mitochondrial fractions were obtained from D10 T cells stimulated with 1 μM thapsigargin for 5 min, or with vehicle, in the presence or absence of 12 mM LNAC. Anti-PKD1 was used to immunoprecipitate DRAK2 and PKD from mitochondrial lysate. *F*, ROS generation through inhibition of mitochondrial complex I using CCCP is sufficient to activate DRAK2. D10 T cells were stimulated with 200 ng/ml PMA, 1 μM thapsigargin or DMSO for 5 min, or CCCP at the indicated times and concentrations. Lysates were resolved by SDS-PAGE and probed with the indicated Abs. *G*, Model for

PKD-dependent DRAK2 activation. TCR stimulation leads to activation of PLCγ, which leads to production of IP_3, and subsequent release of calcium from the ER through IP_3 receptors. ER calcium release allows Orai1 to form functional CRAC channels in the plasma membrane, resulting in a large influx of extracellular calcium, which accelerates mitochondrial respiration and the production of ROS. ROS positively feed back on PLCγ activation and, through Src and Abl, can activate PKD. PKD, following activation through potentially one of these pathways, is then able to activate DRAK2, which serves to limit calcium influx.